Stable internal dynamics of a legged hopping model with locomotion speed control

Ambrus Zelei[1,2], László Bencsik[1,2], Tamás Insperger[2,3], and Gábor Stépán[1,3]

[1] MTA-BME Research Group on Dynamics of Machines and Vehicles, Budapest,H-1111, Hungary
zelei@mm.bme.hu,
[2] MTA-BME Lendület Human Balancing Research Group, Budapest,H-1111, Hungary
bencsik@mm.bme.hu,
[3] Department of Applied Mechanics, Budapest University of Technology and Economics
insperger@mm.bme.hu, stepan@mm.bme.hu

Abstract. The dynamic analysis of legged locomotion typically involves issues related to multibody dynamics, underactuation, motion planning and stability. In addition to biomechanics of humans and animals, the dynamic analysis of legged locomotion is also an important issue in the control development of pedal robots. For these robots, stable internal dynamics has to be guaranteed in order to achieve reliable control.
The goal of this study is the conceptual proof of a direct eigenvalue analysis method for the internal dynamics of legged robotic locomotors. The starting point is a planar model of hopping, which provides stable periodic motion without the feedback control of the locomotion speed. In the present study, we extend the existing model with a controller whose goal is to zero the virtual constraint related to the prescribed locomotion speed. We expect that the locomotion speed can be set arbitrarily in a certain range, where the internal dynamics is stable. The stability of the internal dynamics is analyzed using a recently published method based on direct eigenvalue analysis. Although, this method is not usual in control theory, it can efficiently be applied for multibody systems.

Keywords: Pedal locomotion, multibody dynamics, underactuated systems, zero dynamics, piecewise smooth dynamical systems, periodic orbits, eigenvalue analysis.

1 Introduction

The understanding of the dynamics of pedal locomotion is an important task both in biomechanics and in robotics [1–9]. The related models are typically underactuated, since the independent control inputs are less than the number of degrees-of-freedom (DoF). The stability of underactuated systems such as locomotors is guaranteed only if their internal dynamics is stable. One may analyze the internal dynamics by the priory separation of the controlled and

the internal dynamics [10, 11]. However, in this study, we apply an alternative approach which is based on the direct eigenvalue analysis of the system [12].

The legged locomotion is typically split into the flight (airborne) and the ground (stance) phases, which are connected by ground-foot collisions and ground-food detachments [1,3,5,9]. Therefore, the corresponding dynamical models usually belong to the group of *hybrid systems* [3, 13]. Methods for the dynamic analysis of hybrid systems are also utilized in this work.

We demonstrate the direct eigenvalue analysis on a hopping leg model [9], which **1)** provides stable hopping motion and **2)** guarantees the prescribed locomotion speed. The latter control goal, which is achieved by event-based stride-to-stride control decisions [14], is a new development in our model. The control algorithm is time-invariant, so that no precomputed trajectories are needed to realize the motion. The stability of the internal dynamics is achieved by a zero-moment-pole (ZMP) control [4,5], while the locomotion speed control is achieved by a higher level feedback controller.

2 A dynamic model of stable hopping locomotion

The hopping model analysed in this paper consists of the dynamic equations of the underlying multibody system (Sec. 2.1). The dynamic equations are coupled with the equations of the transitions between the ground and flight phases (Sec. 2.2). Furthermore, the control equations form a coherent part of the mathematical model (Sec. 2.3). The control includes a certain set of equations for providing stable hopping similarly as in the previous model in [9]. The control of the locomotion speed is realized in a higher level control, which is a new extension of the model.

2.1 Mechanical structure

The planar mechanical model of our human-like hopping leg is depicted in Fig. 1. The rigid, homogeneous, prismatic segments 1, 2 and 3 correspond to the foot, shank and thigh, respectively. The kinematic pairs A, B, C and D correspond to the tiptoe, the ankle joint, the knee joint and the hip joint, respectively. These are characterized by their masses m_i and lengths l_i, $i = 1, 2, 3$. The overall centre of mass (CoM) location is indicated by G. The upper body is modelled by a reaction wheel with mass m_r. Its moment of inertia with respect to the y-axis through point D is J_r. The input torques are exerted at joints B, C and D, as it is shown on the right of Fig. 1. The actuating torques M_B, M_C and M_D are defined by the control law introduced in Sec. 2.3. Neglecting nonlinear spring characteristics related to the muscle-tendon dynamics [2], muscle torques $k_\mathrm{B}(\theta_{12} - \alpha_{12})$ and $k_\mathrm{C}(\theta_{23} - \alpha_{23})$ are modelled by linear torsional springs of stiffness k_B and k_C, where α_{12} and α_{23} denote the ankle- and knee-joint angles corresponding to the unstretched springs, respectively.

The general coordinates $\mathbf{q} = [x_\mathrm{A}, z_\mathrm{A}, \theta_1, \theta_{12}, \theta_{23}, \theta_\mathrm{r}]^\mathrm{T}$ describe the $n = 6$ DoF system. The Cartesian coordinates of the tiptoe are x_A and z_A in horizontal and

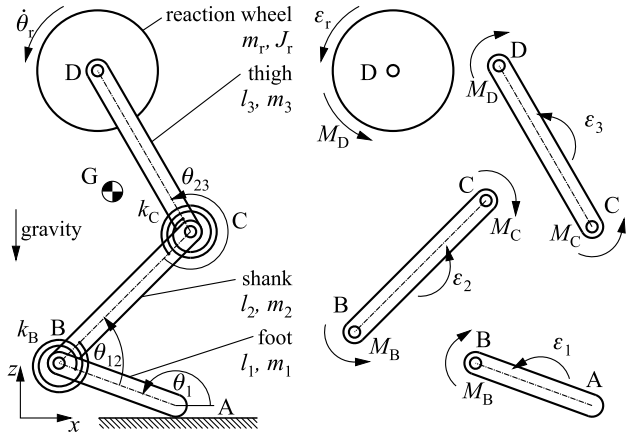

Fig. 1. Segmented leg model with torsional springs, under vertical gravity above a flat, rigid, horizontal ground (left). Free-body-diagram showing control torques (right).

vertical direction, respectively. The foot angle θ_1 is measured from the horizontal, while θ_{12} and θ_{23} are the relative angles of the ankle and the knee. The angular position of the reaction wheel is θ_r. The equation of motion is formulated in the general form

$$\mathbf{H}(\mathbf{q})\ddot{\mathbf{q}} + \mathbf{C}(\mathbf{q}, \dot{\mathbf{q}}) = \mathbf{Q}(\mathbf{q}, \dot{\mathbf{q}}) \,, \tag{1}$$

where $\dot{\mathbf{q}}$ and $\ddot{\mathbf{q}}$ are the vectors of general velocities and accelerations, respectively. The mass matrix is $\mathbf{H} \in \mathbb{R}^{n \times n}$, and vector $\mathbf{C} \in \mathbb{R}^n$ contains the centrifugal and Coriolis forces. The gravitational forces, the torques of the torsional springs and the control torques are collected in the general force vector $\mathbf{Q} \in \mathbb{R}^n$.

2.2 Flight and ground phase transitions

In the airborne phase, the system has 6 DoFs, while, in the stance phase, the tiptoe is fixed to the ground. In order to use the first order form of the dynamic equations we introduce the state variable vector $\mathbf{x} = [\mathbf{q},\, \dot{\mathbf{q}}]^{\mathrm{T}}$, where $\mathbf{x} \in \mathbb{R}^{2n}$. The dynamic equation (1) of the flight and ground phases are reformulated as

$$\dot{\mathbf{x}}(t) = \mathbf{f}_{\mathrm{F}}(\mathbf{x}(t)), \qquad \dot{\mathbf{x}}(t) = \mathbf{f}_{\mathrm{G}}(\mathbf{x}(t)) \tag{2}$$

respectively, where

$$\mathbf{f}_{\mathrm{F}}(\mathbf{x}(t)) = \begin{bmatrix} \dot{\mathbf{q}} \\ -\mathbf{H}^{-1}(\mathbf{C} - \mathbf{Q}) \end{bmatrix}, \qquad \mathbf{f}_{\mathrm{G}}(\mathbf{x}(t)) = \begin{bmatrix} \mathbf{0}_{2\times 1} \\ \dot{\mathbf{q}}_{\mathrm{red}} \\ \mathbf{0}_{2\times 1} \\ -\mathbf{H}_{\mathrm{red}}^{-1}(\mathbf{C}_{\mathrm{red}} - \mathbf{Q}_{\mathrm{red}}) \end{bmatrix} \tag{3}$$

are smooth vector fields. Due to the constraint provided by fixing the tiptoe to the ground, the reduced general velocity vector $\dot{\mathbf{q}}_{\mathrm{red}} = [\dot{\theta}_1, \dot{\theta}_{12}, \dot{\theta}_{23}, \dot{\theta}_{\mathrm{r}}]^{\mathrm{T}}$ is

applied in the ground phase. Similarly, the reduced mass matrix $\mathbf{H}_{\mathrm{red}}$ is obtained by truncating the first two rows and columns of $\mathbf{H}$, while $\mathbf{C}_{\mathrm{red}}$ and $\mathbf{Q}_{\mathrm{red}}$ are obtained by truncating the first two rows of $\mathbf{C}$ and $\mathbf{Q}$, respectively. The vector field $\mathbf{f}_{\mathrm{G}}$ results that the acceleration and velocity components of the tiptoe are $\ddot{x}_{\mathrm{A}} = 0$, $\ddot{z}_{\mathrm{A}} = 0$ and $\dot{x}_{\mathrm{A}} = 0$, $\dot{z}_{\mathrm{A}} = 0$ respectively.

Flight to ground (F2G) The flight to ground transition happens when the switching surface Σ_{F2G}, defined by

$$h_{\mathrm{F2G}}(\mathbf{x}) := z_{\mathrm{A}} = 0 \tag{4}$$

is crossed. Technically, the switching surface Σ_{F2G} is the ground itself in the present model. The F2G transition includes the collision of the foot with the ground. The collision is completely inelastic and instantaneous and there is no rebound [6, 7, 9]. Our further assumption is that the friction force prevents the slip of the foot [8]. All in all, the velocities $\dot{x}_{\mathrm{A}}$ and $\dot{z}_{\mathrm{A}}$ become zero and the angular velocities have discontinuities too when the solution reaches Σ_{F2G}. This abrupt change of the general velocities in $\dot{\mathbf{q}}$ is described by the jump function:

$$\mathbf{g}_{\mathrm{F2G}}(\mathbf{x}) = \begin{bmatrix} \mathbf{q} \\ (\mathbf{I}_{n\times n} - \mathbf{P}_{\mathrm{c}})\dot{\mathbf{q}} \end{bmatrix}. \tag{5}$$

The mapping $\mathbf{g}_{\mathrm{F2G}}(\mathbf{x})$ specifies the post-impact location of the solution, with the projection of the velocities into the direction which is admissible by the physical constraints $\boldsymbol{\gamma}(\mathbf{q})$ [15, 16]. The projection can be formulated as:

$$\mathbf{P}_{\mathrm{c}} = \mathbf{H}^{-1}\boldsymbol{\gamma}_{\mathbf{q}}^{\mathrm{T}}(\boldsymbol{\gamma}_{\mathbf{q}}\mathbf{H}^{-1}\boldsymbol{\gamma}_{\mathbf{q}}^{\mathrm{T}})^{-1}\boldsymbol{\gamma}_{\mathbf{q}}. \tag{6}$$

Ground to flight (G2F) The ground to flight transition at the surface Σ_{G2F}, defined by

$$h_{\mathrm{G2F}}(\mathbf{x}) := \lambda_z = 0, \tag{7}$$

is a switch from the smooth vector field $\mathbf{f}_{\mathrm{G}}$ to $\mathbf{f}_{\mathrm{F}}$ (see (2)) without any discontinuity of the solution. In (7), the Lagrange multiplier represents the magnitude of the contact force and the positive sign of λ_z refers to a pulling force. The mathematical form of the corresponding jump function is

$$\mathbf{g}_{\mathrm{G2F}}(\mathbf{x}) = \mathbf{x}. \tag{8}$$

The contact force $\boldsymbol{\lambda}$ is calculated by evaluating following expression

$$\begin{bmatrix} \ddot{\mathbf{q}} \\ \boldsymbol{\lambda} \end{bmatrix} = \begin{bmatrix} \mathbf{H}(\mathbf{q}) & \boldsymbol{\gamma}_{\mathbf{q}}^{\mathrm{T}}(\mathbf{q}) \\ \boldsymbol{\gamma}_{\mathbf{q}}(\mathbf{q}) & \mathbf{0} \end{bmatrix}^{-1} \begin{bmatrix} \mathbf{Q}(\mathbf{q},\dot{\mathbf{q}}) - \mathbf{C}(\mathbf{q},\dot{\mathbf{q}}) \\ -\dot{\boldsymbol{\gamma}}_{\mathbf{q}}(\mathbf{q},\dot{\mathbf{q}})\dot{\mathbf{q}} \end{bmatrix} \tag{9}$$

with the already calculated values of $\mathbf{q}$ and $\dot{\mathbf{q}}$. The expression in (9) is identical with the from-3-to-1 index reduction scheme of differential algebraic equations in [17]. The Jacobian of the constraint vector is $\boldsymbol{\gamma}_{\mathbf{q}}(\mathbf{q}) = \partial\boldsymbol{\gamma}(\mathbf{q})/\partial\mathbf{q}$ and the ground-foot contact is represented by $\boldsymbol{\gamma}(\mathbf{q}) = \mathbf{0}$ with

$$\boldsymbol{\gamma}(\mathbf{q}) = \left[x_{\mathrm{A}}\,, z_{\mathrm{A}}\right]^{\mathrm{T}}. \tag{10}$$

2.3 Internal dynamics stabilization and locomotion speed control

The time-dependent and time-invariant control concepts of legged locomotion are clearly distinguished in [4, 5]. In case of time-dependent control approaches the control goal is the tracking of precomputed trajectories. However, our concept fits better into the group of time-invariant approaches, when the control actions are driven by the events along the motion of the locomotor. The control goal is the stable gait generation; and additionally, the nominal locomotion speed is prescribed without the tracking of any prescribed trajectories.

Stable gait generation The required control torques are formalized separately for the flight ((11)-(13)) and ground ((15)-(17)) phase. The control torques $M_{\mathrm{B}}^{\mathrm{F}}$ and $M_{\mathrm{C}}^{\mathrm{F}}$ play the role of dampers. The horizontal position x_{A} of the tiptoe relative to the nominal horizontal position $x_{\mathrm{G}} + x_{\Delta}$ is maintained by the proportional-derivative (PD) controller realized by torque $M_{\mathrm{D}}^{\mathrm{F}}$. The torques $M_{\mathrm{B}}^{\mathrm{F}}$, $M_{\mathrm{C}}^{\mathrm{F}}$ and $M_{\mathrm{D}}^{\mathrm{F}}$ are given by

$$M_{\mathrm{B}}^{\mathrm{F}} = -D_{\mathrm{B}}\dot{\theta}_{12}\,, \tag{11}$$

$$M_{\mathrm{C}}^{\mathrm{F}} = -D_{\mathrm{C}}\dot{\theta}_{23}\,, \tag{12}$$

$$M_{\mathrm{D}}^{\mathrm{F}} = P(x_{\mathrm{A}} - (x_{\mathrm{G}} + x_{\Delta})) + D(\dot{x}_{\mathrm{A}} - \dot{x}_{\mathrm{G}})\,, \tag{13}$$

where D_{B}, D_{C}, P and D are control gains. We emphasize, that the CoM position x_{G} is not precomputed, but obtained from the actual state. In order to achieve a ZMP control [4, 5], the value x_{Δ} in the nominal tiptoe position is given by

$$x_{\Delta} = P_{\Pi}\,\Pi_{\mathrm{A}} - K_v\,, \tag{14}$$

where Π_{A} is the angular momentum about the point A, P_{Π} is an associated control gain and K_v is a control parameter responsible for tuning the locomotion speed. We note that the pre-impact positioning of the tiptoe is considered as the foot touchdown preparation.

In the stance phase, the mechanical energy level is maintained by means of the control torques at the ankle and the knee (see Eqs. (15), (16)). The control goal is the zeroing the difference of the total mechanical energy E and the target energy level E_0, which is arbitrarily chosen in the stable range. The torque $M_{\mathrm{D}}^{\mathrm{G}}$ in (17) plays the role of a spring and a viscous damper and therefore prevents the continuous growth of the angular velocity $\dot{\theta}_{\mathrm{r}}$. The control torques of the ground phase are given by

$$M_{\mathrm{B}}^{\mathrm{G}} = P_E(E - E_0)\,\mathrm{sgn}(\dot{\theta}_{12})\,, \tag{15}$$

$$M_{\mathrm{C}}^{\mathrm{G}} = P_E(E - E_0)\,\mathrm{sgn}(-\dot{\theta}_{23})\,, \tag{16}$$

$$M_{\mathrm{D}}^{\mathrm{G}} = -P_{\mathrm{r}}\theta_{\mathrm{r}} - D_{\mathrm{r}}\dot{\theta}_{\mathrm{r}}\,, \tag{17}$$

where P_E, P_{r} and D_{r} are control gains.

The torques in (11)-(17) are supposed to guarantee the stability of the internal dynamics, i.e. the periodicity of the motion. The tuning of the parameters in (11)-(17) are based on the investigation of the stability of the internal dynamics [10] as detailed in Sec. 3.

Maintenance of the locomotion speed Besides the stable gait, an additional control goal is to keep the prescribed average locomotion speed, which is achieved by zeroing the following virtual constraint $\sigma \in \mathbb{R}^1$:

$$\sigma = x_{\mathrm{G}}(t+T) - x_{\mathrm{G}}(t) - Tv^{\mathrm{d}}, \tag{18}$$

where x_{G} describes the horizontal position of the CoM and T is the time period. Equation (18) is the generalization of the so-called servo-constraint (virtual holonomic constraint) [18]. The servo-constraint in the original sense is a function of the current state variables. However, (18) includes the motion for the whole period: $\dot{x}_{\mathrm{G}}(t)$ is integrated over the interval $[t,\, t+T]$. The output (18) is evaluated once in each period.

The output (18) is guaranteed by a higher level feedback controller that performs the stride-to-stride modification of K_v, which is a gain parameter in the low level controller (13). In order to have a compact form of the mathematical description of the whole dynamics, the gain parameter K_v is maintained as a state variable. The dynamics of K_v is defined in the flight and ground phase by

$$\dot{K_v}(t) = \mathbf{f}_{\mathrm{F}}^{K_v}(K_v(t)), \qquad \dot{K_v}(t) = \mathbf{f}_{\mathrm{G}}^{K_v}(K_v(t)) \tag{19}$$

respectively, where the smooth vector fields $\mathbf{f}_{\mathrm{F}}^{K_v} \in \mathbb{R}^1$ and $\mathbf{f}_{\mathrm{G}}^{K_v} \in \mathbb{R}^1$ are defined as

$$\mathbf{f}_{\mathrm{F}}^{K_v}(K_v(t)) = [0], \qquad \mathbf{f}_{\mathrm{G}}^{K_v}(K_v(t)) = [0]. \tag{20}$$

The gain K_v does not change during the continuous phases. The value of the gain K_v is updated at the end of each period which is in coincidence with the time instance of the G2F transition. The corresponding $\mathbb{R}^1$ jump functions are

$$\mathbf{g}_{\mathrm{F2G}}^{K_v}(K_v) = [K_v] \tag{21}$$

$$\mathbf{g}_{\mathrm{G2F}}^{K_v}(K_v) = [K_v - P_\sigma \sigma] \tag{22}$$

where σ is the control output defined in (18) and P_σ is the associated positive control gain. Equation (22) realizes the feedback for the locomotion speed control. Based on (18) and (22), the controller performs stride-to-stride control decision which is typical in time-invariant control approaches [5].

3 Stability analysis of the internal dynamics

The stability analysis of the internal dynamics [10] is necessary when stable control is designed. We apply the direct eigenvalue analysis detailed in [12].

3.1 A compact mathematical formulation

In order to obtain a compact mathematical form, we couple the state variables $\hat{\mathbf{x}} \in \mathbb{R}^{\hat{n}}$ (with $\hat{n} = 2n+1$) and the dynamic equations (2) and (19) of the mechanical system and the feedback control as

$$\hat{\mathbf{x}} = \begin{bmatrix} \mathbf{x} \\ K_v \end{bmatrix}, \qquad \dot{\hat{\mathbf{x}}}(t) = \hat{\mathbf{f}}_{\mathrm{F}}(\hat{\mathbf{x}}(t)), \qquad \dot{\hat{\mathbf{x}}}(t) = \hat{\mathbf{f}}_{\mathrm{G}}(\hat{\mathbf{x}}(t)) \tag{23}$$

respectively, where the smooth vectorfields $\hat{\mathbf{f}}_{\mathrm{F}}(\hat{\mathbf{x}}(t)) \in \mathbb{R}^{\hat{n}}$ and $\hat{\mathbf{f}}_{\mathrm{G}}(\hat{\mathbf{x}}(t)) \in \mathbb{R}^{\hat{n}}$ are

$$\hat{\mathbf{f}}_{\mathrm{F}}(\hat{\mathbf{x}}(t)) = \begin{bmatrix} \mathbf{f}_{\mathrm{F}}(\mathbf{x}(t)) \\ \mathbf{f}_{\mathrm{F}}^{K_v}(K_v(t)) \end{bmatrix}, \qquad \hat{\mathbf{f}}_{\mathrm{G}}(\hat{\mathbf{x}}(t)) = \begin{bmatrix} \mathbf{f}_{\mathrm{G}}(\mathbf{x}(t)) \\ \mathbf{f}_{\mathrm{G}}^{K_v}(K_v(t)) \end{bmatrix}. \tag{24}$$

We also put together the jump functions (5) with (21) and (8) with (22) for the F2G and G2F transitions respectively:

$$\hat{\mathbf{g}}_{\mathrm{F2G}}(\hat{\mathbf{x}}) = \begin{bmatrix} \mathbf{g}_{\mathrm{F2G}}(\mathbf{x}) \\ \mathbf{g}_{\mathrm{F2G}}^{K_v}(K_v) \end{bmatrix}, \qquad \hat{\mathbf{g}}_{\mathrm{G2F}}(\hat{\mathbf{x}}) = \begin{bmatrix} \mathbf{g}_{\mathrm{G2F}}(\mathbf{x}) \\ \mathbf{g}_{\mathrm{G2F}}^{K_v}(K_v) \end{bmatrix}. \tag{25}$$

The illustration of the solution of the resulting $\hat{n} = 2n + 1$ dimensional hybrid dynamical system is depicted in Fig. 2. The dashed curves show a solution for $\mathbf{x}(t)$ and $K_v(t)$ with a general initial condition, and the continuous curves show the periodic solutions $\mathbf{x}^*(t)$ and $K_v^*(t)$.

3.2 Direct analysis of the internal dynamics

We shortly overview the analysis of internal dynamics in case of our dynamic system, which is $\hat{n}$ dimensional with the state vector $\hat{\mathbf{x}}$. The output σ in (18) is one dimensional, therefore the *relative degree* r [10,19] is a scalar, which defines the input-output relation. Based on the *partial feedback linearization* [10,19], the control problem can be described with r number of states in general: if $r < \hat{n}$, then $\hat{n} - r$ number of states is not necessary for the exact definition of the output. In such case the full state input-output linearization is not possible and the *internal dynamics* of $\hat{n} - r$ dimensions exists [10]. The related unobservable

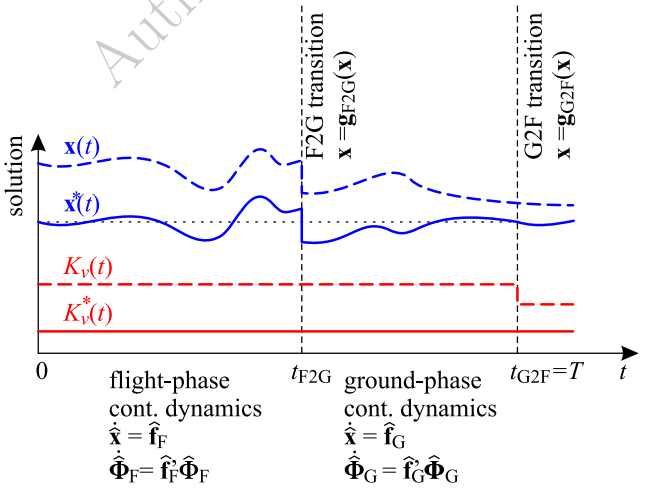

Fig. 2. The piecewise smooth solution for the general coordinates and velocities $\mathbf{x}$ and the gain parameter K_v.

states cannot be seen from the input-output relationship. Besides, the *controlled dynamics* of dimensions r can be separated by the partial feedback linearization.

In what follows, a recently published method is applied [12]. This method eliminates the need of the a priori transformation of the system into controlled and internal dynamics. The method in [12] is based on the direct eigenvalue analysis technique of differential algebraic systems. The method in [12] utilizes that the equation of motion is subjected to servo-constraints. Regarding the servo-constraint, the restricted and the admissible directions can be distinguished in the state space. Free motion is possible only in the admissible direction and it belongs to the internal dynamics [12].

The above explained idea is applied for the eigenvalue analysis of the *monodromy matrix* of our hybrid hopping system. Assuming that the relative periodic orbit is found with a shooting approach, we apply the *first variational equation* in the following form separately for the flight and the grounded phase for the calculation of the fundamental solution matrices [3, 13, 16] $\hat{\boldsymbol{\Phi}}_{\mathrm{F}}(t)$ and $\hat{\boldsymbol{\Phi}}_{\mathrm{G}}(t)$:

$$\dot{\hat{\boldsymbol{\Phi}}}_{\mathrm{F}}(t) = (\nabla_{\hat{\mathbf{x}}} \hat{\mathbf{f}}_{\mathrm{F}}(\hat{\mathbf{x}}))\hat{\boldsymbol{\Phi}}_{\mathrm{F}}(t), \qquad \dot{\hat{\boldsymbol{\Phi}}}_{\mathrm{G}}(t) = (\nabla_{\hat{\mathbf{x}}} \hat{\mathbf{f}}_{\mathrm{G}}(\hat{\mathbf{x}}))\hat{\boldsymbol{\Phi}}_{\mathrm{G}}(t) \tag{26}$$

with initial conditions $\hat{\boldsymbol{\Phi}}_{\mathrm{F}}(0) = \mathbf{I}$ and $\hat{\boldsymbol{\Phi}}_{\mathrm{G}}(0) = \mathbf{I}$. Here $\mathbf{I}$ is the $\mathbb{R}^{\hat{n}\times\hat{n}}$ identity matrix. The solution Jacobian $\hat{\boldsymbol{\Phi}}(t)$ which is also referred as *monodromy matrix*, is then obtained for the entire relative periodic orbit by the composition

$$\hat{\boldsymbol{\Phi}}(t_{\mathrm{G2F}}) = \hat{\mathbf{S}}_{\mathrm{G2F}}\, \hat{\boldsymbol{\Phi}}_{\mathrm{G}}(t_{\mathrm{G2F}})\, \hat{\mathbf{S}}_{\mathrm{F2G}}\, \hat{\boldsymbol{\Phi}}_{\mathrm{F}}(t_{\mathrm{F2G}}). \tag{27}$$

Here, matrices $\hat{\mathbf{S}}_{\mathrm{G2F}}$ and $\hat{\mathbf{S}}_{\mathrm{F2G}}$ describe the contribution of the mappings at the phase transitions, which are known as the *saltation matrices*. The saltation matrices are determined based on [3, 16]. The stability of the relative periodic orbit is determined from the eigenvalues μ_i $(i = 1 \dots \hat{n})$ of the monodromy matrix $\hat{\boldsymbol{\Phi}}(t_{\mathrm{G2F}})$, which are known as the *Floquet-multipliers* [13].

The identification of the Floquet-multiplier related to the controlled motion is achieved by the local sensitivity analysis regarding the feedback parameter P_σ. The remaining $\hat{n} - 1$ number of Floquet-multipliers are related to the internal dynamics. For the local sensitivity analysis, the partial derivatives of all μ_i Floquet multipliers are calculated with respect to P_σ. The resulting Jacobian assumes the form

$$\mathbf{T} = \left[\frac{\partial \mu_1}{\partial P_\sigma} \cdots \frac{\partial \mu_{\hat{n}}}{\partial P_\sigma} \right]. \tag{28}$$

In practice this matrix can be constructed with numerical differentiation. Here the largest elements of the Jacobian $\mathbf{T}$ are associated with the controlled dynamics and the remaining eigenvalues are associated with the internal dynamics.

4 Results

Forward hopping (case A), hopping on the spot (case B) and backward hopping (case C) are investigated as shown in Fig. 3. For all the three cases, five hops are simulated which is shown by the periodic blue and red curves, which show the

path of the CoM and the tiptoe, respectively. The stroboscopic view of the model is shown for each period in different phase shifts. The internal dynamics, which is related to the periodic hopping, was stable as the simulation results show: the hopping height and the velocity was uniform in each period. Furthermore, the controller maintains the locomotion speed defined as an output by (18).

5 Conclusions

We applied a novel sensitivity based direct eigenvalue analysis for the investigation of the stability of the internal dynamics of an underactuted hopping model. The internal dynamics related to the hopping motion was stable and the locomotion speed was guaranteed by the controller. The results were demonstrated by numerical simulations and will be applied in further research related to legged locomotion dynamics.

Acknowledgement

This work was supported by the Hungarian National Research, Development and Innovation Office (Project id.: NKFI-FK18 128636) and by the Higher Education Excellence Program of the Ministry of Human Capacities in the frame of Biotechnology research area of Budapest University of Technology and Economics (BME FIKP-BIO).

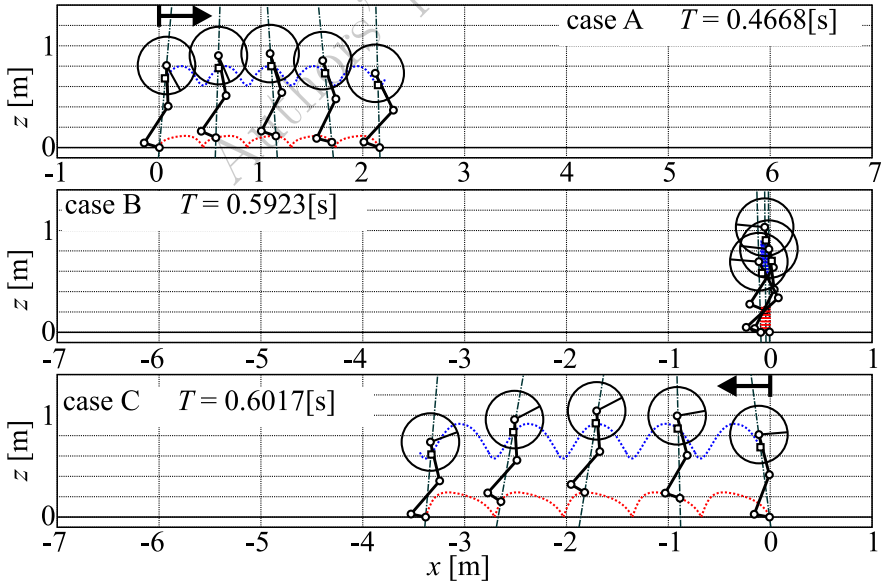

Fig. 3. Simulation results for forward hopping, hopping on the spot and backward hopping

References

1. T. F. Novacheck. The biomechanics of running. *Gait and Posture*, 7:77–95, 1998.
2. A. Seyfarth, M. Günther, and R. Blickhan. Stable operation of an elastic three-segment leg. *Biol Cybern.*, 84(5):365–382, 2001.
3. P. T. Piiroinen and H. J. Dankowicz. Low-cost control of repetitive gait in passive bipedal walkers. *International Journal of Bifurcation and Chaos*, 15(6):1959–1973, 2005. doi:10.1142/S0218127405013083.
4. P. Holmes, R. J. Full, D. E. Koditschek, and J. Guckenheimer. The dynamics of legged locomotion: Models, analyses, and challenges. *SIAM Rev.*, 48(2):207–304, 2006.
5. Eric R. Westervelt, Jessy W. Grizzle, Christine Chevallereau, and et al. Feedback control of dynamic bipedal robot locomotion, 2007.
6. D. E. Lieberman, M. Venkadesan, W. A. Werbel, A. I. Daoud, S. D'Andrea, I. Davis I., I. S. Mang'Eni, and Y. Pitsiladis. Foot strike patterns and collision forces in habitually barefoot versus shod runners. *Naure, Biomechanics*, 463(8723):531–535, 2010.
7. J. Kövecses and L. L. Kovács. Foot impact in different modes of running: mechanisms and energy transfer. *Procedia IUTAM*, 2:101–108, Symposium on Human Body Dynamics, 2011.
8. J. M. Font-Llagunes, R. Pamies-Vila, and J. Kövecses. Configuration-dependent performance indicators for the analysis of foot impact in running gait. In *Proceedings of ECCOMAS Thematic Conference on Multibody Dynamics, Multibody Dynamics 2013, Book of Abstracts*, pages 31–32, Zagreb, Croatia, 1-4 July.
9. A. Zelei, B. Krauskopf, and T. Insperger. Control optimization for a three-segmented hopping leg model of human locomotion. In *DSTA 2017 – Vibration, Control and Stability of Dynamical Systems*, pages 599–610, Lodz, Poland, 11-14, December 2017.
10. J. J. E. Slotine and W. Li. *Applied Nonlinear Control*. Prentice Hall, 1995.
11. A. Isidori. *Nonlinear control systems, 3rd edition*. Springer-Verlag, London, 1995.
12. L. Bencsik, L.L. Kovács, and A. Zelei. Stabilization of internal dynamics of underactuated systems by periodic servo-constraints. *International Journal of Structural Stability and Dynamics*, 2017. 14 pages, paper id: 1740004.
13. R. I. Leine and D. H. van Campen. Discontinuous bifurcations of periodic solutions. *Mathematical and Computer Modelling*, 36(3):259–273, 2002. doi:10.1016/S0895-7177(02)00124-3.
14. W. B. Bequette. *Process control: Modeling, design, and simulation*. Prentice Hall Professional, New Jersey, 2003.
15. J. Kövecses, J.-C. Piedoboeuf, and C. Lange. Dynamic modeling and simulation of constrained robotic systems. *IEEE/ASME Transactions on Mechatronics*, 2(2):165–177, 2003.
16. H. J. Dankowicz and P. T. Piiroinen. Exploiting discontinuities for stabilization of recurrent motions. *Dynamical Systems*, 17(4):317–342, 2002. doi:/10.1080/1468936021000041663.
17. R. L. Petzold. Recent developments in the numerical solution of differential/algebraic systems. *Computer Methods in Applied Mechanics and Engineering*, 36(6):77–89, 2002.
18. V. I. Kirgetov. The motion of controlled mechanical systems with prescribed constraints (servo constraints). *Prikl. Mat. Mekh.*, 31(3):433–447, 1967.
19. Isidori A. *Nonlinear Control Systems*. 3rd ed. Springer Verlag, 1995.